UCRL-TR-209718

LAWRENCE
LIVERMORE
NATIONAL
LABORATORY

Gen IV Nuclear Energy Systems Interim Status Report on Pre-conceptual LFR Design Studies and Evaluations

W. G. Halsey, N. W. Brown, C. F. Smith, J. J. Sienicki, A. V. Moisseytsev, S. J. Kim, M. A. Smith, W. S. Yang, M. Williamson, N. Li

February 15, 2005

This work was performed under the auspices of the U.S. Department of Energy by University of California, Lawrence Livermore National Laboratory under Contract W-7405-Eng-48.

UCRL-TR-209718

Generation IV Nuclear Energy Systems

Interim Status Report

On Pre-conceptual LFR Design Studies and Evaluations

January 31, 2005

Office of Advanced Nuclear Research

DOE Office of Nuclear Energy, Science and Technology

Interim Status Report
On Pre-conceptual LFR Design Studies and Evaluations

Introduction

This document is a report of the status of work in progress within the Generation-IV Nuclear Technology Lead-Cooled Fast Reactor program. It is primarily a report of results from recent reactor design studies conducted at ANL, but includes a summary of ongoing work in the areas of coolant and materials studies, systems studies and international cooperation by other participants. Input has been received from all Gen-IV LFR program participants as noted throughout the text.

The Generation-IV Lead-cooled Fast-spectrum Reactors (LFR) Program is conducting research[1] into small transportable long core-life fast-spectrum reactors that use liquid lead (Pb) or lead-bismuth eutectic (LBE) coolant. A phased program of reactor design, system definition and materials studies is planned to support a decision on construction of a demonstration system within ten years.

Contributing Authors:

Argonne National Lab

James J. Sienicki
Anton V. Moisseytsev
Sang Ji Kim
Michael A. Smith
Won Sik Yang
Mark Williamson

Los Alamos National Lab

Ning Li

Lawrence Livermore National Lab

Neil W. Brown
William G. Halsey
Craig F. Smith

Reference

1) "Development Plan for the Small, Secure, Transportable, Autonomous Reactor (SSTAR)", C. F. Smith, N. W. Brown, W. G. Halsey (Lawrence Livermore National Laboratory), D. C. Crawford, D. C. Wade (Argonne National Laboratory), M. W. Cappiello, N. Li (Los Alamos National Laboratory), UCRL-ID-153961, Lawrence Livermore National Laboratory, Livermore, CA, July 2003.

Status Report on Pre-conceptual LFR Design Studies:

J. Sienicki, A. Moisseytsev, S. Kim, M. Smith, W. Yang, (ANL)

1.0 INTRODUCTION

Previous pre-conceptual core neutronics and system thermal hydraulics calculations initiated the investigation of viability of a Small Secure Transportable Autonomous Reactor (SSTAR) lead-cooled small modular fast reactor concept.[1] The calculations indicated that a single-phase natural circulation SSTAR reactor concept with good core reactor physics performance, good system thermal hydraulics performance, and a high Supercritical Carbon Dioxide (S-CO_2) Brayton cycle efficiency of 40 % may be viable at an electrical power of 18 MWe (45 MWt).

Pre-conceptual studies of SSTAR viability have continued with the objective of improving the system thermal hydraulic performance and raising the plant efficiency as well as extending the neutronics analysis. This effort has been motivated by several considerations. First, the initial Pre-conceptual studies were focused upon a "pancake" core having a height-to-diameter of 0.5. It was found that a compact core with high average burn up could be realized with a height-to-diameter ratio of 0.8. Second, the initial assumed reactor vessel height of 12.2 meters limited the height of the Pb-to-CO_2 in-reactor heat exchangers (HXs) which reduced the efficiency of supercritical carbon dioxide (S-CO_2) Brayton cycle power converter. It was found that by increasing the reactor vessel height to 18 meters, the greater driving head for single-phase natural circulation would offset both the greater pressure drop of the 0.8 height-to-diameter ratio core as well as the pressure drop of taller HXs. This has enabled the plant efficiency to be increased from 40 to 43 % and the plant electrical power to be raised from 18 to 20 MWe. Third, reactivity feedback coefficients, which had previously not been generated for SSTAR, have now been calculated for the core. The reactivity feedback coefficients provide a basis for future investigation of the autonomous load following and passive shutdown behavior of the reactor. The current status of SSTAR and the Pre-conceptual viability studies are described below.

2.0 KEY FEATURES OF SSTAR

Key features incorporated in SSTAR include:

- Proliferation resistance:
  - Core lifetime/refueling interval of 20 years;
  - Core is a single cassette and is not composed of individual removable fuel assemblies;
  - Restricted access to fuel during the core lifetime;
  - Refueling equipment is present at the site only during refueling operations at the end of the core lifetime;
  - Transuranic fuel which is self protective in the safeguards sense;

- Molten lead (Pb) primary coolant and nitride fuel:
  - Passive safety and potential to operate at higher system temperatures than traditional liquid metal cooled fast reactors;
- Autonomous operation:
  - Core power adjusts itself to heat demand from the reactor system due to large inherent reactivity feedbacks of the fast spectrum core without operator motion of control rods;
  - Active adjustment of shutdown rods for startup and shutdown, and compensation rods for burn up compensation over the core lifetime;
- Fissile self-sufficiency:
  - Conversion ratio near unity;
  - Realization of a sustainable closed fuel cycle;
- Supercritical carbon dioxide (S-CO_2) gas turbine Brayton cycle power converter:
  - Higher plant efficiency than Rankine saturated steam cycle at the same temperature;
  - Reduced balance of plant footprint, costs, and staffing requirements;
- Natural circulation primary coolant heat transport:
  - Eliminates main coolant pumps and loss-of-flow accidents;
- Factory fabrication:
  - All reactor and balance of plant components including reactor and guard vessels;
  - Reduced costs and improved quality control;
- Factory assembly of components into transportable modules:
  - Short modular installation and assembly times at site;
- Full transportability by barge or rail, or possibly by road;
- Flexibility to be adapted to generate other energy products:
  - Desalinated water or hydrogen.

The use of lead coolant enhances passive safety. Lead is chemically inert; that is, it does not react chemically with the CO_2 working fluid above ~ 250 °C. Lead does not react vigorously with air or water/steam. Lead has a high boiling temperature of 1740 °C (1670 °C for Pb-Bi eutectic). *As a consequence, under all operational transients and postulated accidents, the SSTAR core and heat exchangers remain covered by ambient pressure single-phase primary coolant and single-phase natural circulation removes the core power.*

The use of nitride fuel also enhances passive safety. Nitride has a high melting temperature (> 2600 °C for UN) as well as a high temperature for decomposition (> 1400 °C for mixed nitride). Its high thermal conductivity together with the Pb bond between the fuel pellets and cladding reduce the fuel-coolant temperature difference. Nitride is compatible with a fast neutron spectrum and provides a high atom density. The nitrogen is enriched in N^{15} to eliminate parasitic reactions in N^{14} and waste disposal problems associated with C^{14} production. In addition, nitride fuel is compatible with both the ferritic-martensitic stainless steel cladding and Pb coolant; nitrogen is insoluble in Pb. Molten Pb bonds the nitride pellets to the cladding. Nitride further offers low irradiation-induced swelling and fission gas release.

The lead coolant and nitride fuel together provide the potential to operate the LFR reactor system at higher temperatures than traditional liquid metal-cooled fast reactors. A peak cladding temperature of 650 °C is assumed as an upper limit in the present analysis.

3.0 SUMMARY OF NEUTRONICS ANALYSES

A power level of 20 MWe (45 MWt) is chosen because it is an optimal value for an assumed compact core with a core fuel volume fraction that allows natural circulation heat transport at nominal power. A 20-year core life, fixed fuel volume fraction of 0.55, fuel smeared density of 85 %, and core height-to-diameter ratio of 0.8 are assumed. Transuranic (TRU) fuel feed from LWR spent fuel following a 25-year cooling time is assumed. This allows for decay of the Pu^{241} isotope. The core incorporates five distinct TRU enrichment zones including a central low-enrichment region to reduce the peak-to-average power ratio and burn up reactivity swing. The assumed fuel volume fraction of 0.55 is high, but when combined with a large pin diameter, it is shown in the thermal hydraulics analysis below to be low enough to facilitate natural circulation heat transport from the core to the in-vessel Pb-to-CO_2 heat exchangers (HXs).

Given a fixed core power level, Figure 1 shows the results of calculations of the average discharge burn up and burn up reactivity swing versus active core diameter for a simplified cylindrical core geometry (height-to-diameter ratio=0.8) assuming a fuel volume fraction of 0.55 and an 85 % nitride fuel smeared density. It is desired to limit the burn up reactivity swing over the core lifetime to less than one dollar. It is observed that for a fuel volume fraction of 0.55, the burn up reactivity swing exhibits a minimum at an active core diameter of about 1.0 m. Figure 2 plots the average discharge burn up as well as the peak fast fluence versus the active core diameter. Increasing the core thermal power directly increases the average discharge burn up. However, the maximum power is limited by the requirement that the peak fast fluence remain below the assumed limit of 4.0×10^{23} neutrons/cm^2. This limitation is encountered for core powers of about 45 to 50 MWt. Thus, for the assumed 0.55 fuel volume fraction, a core diameter of about 1.0 m minimizes the burn up reactivity swing and a power level of about 45 MWt maximizes the average discharge burn up. More detailed calculations were performed using the DIF3D/REBUS-3 code package. Table 1 shows core conditions and the calculated core neutronics performance.

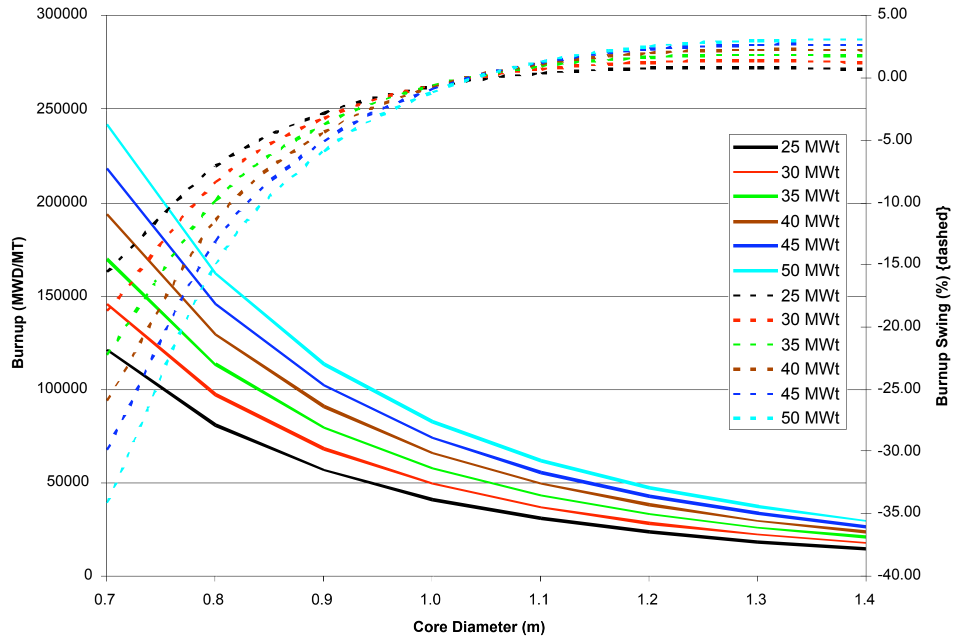

Figure 1. Average Discharge Burn up and Burn up Reactivity Swing versus Active Core Diameter.

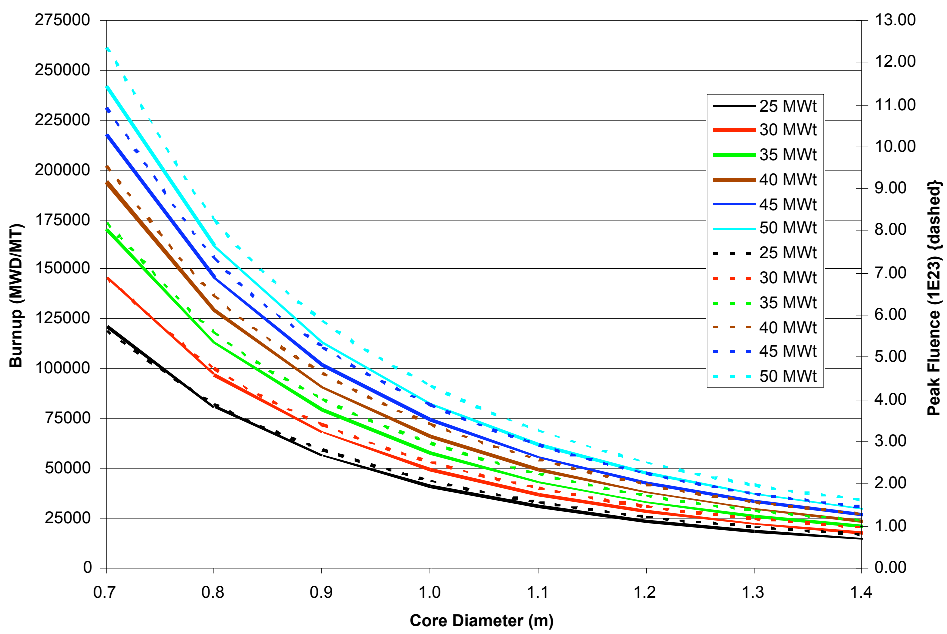

Figure 2. Average Discharge Burn up and Peak Fast Fluence versus Active Core Diameter.

The reference fuel form consists of nitride pellets bonded by molten Pb to silicon-enhanced ferritic-martensitic stainless steel cladding. The fuel pins are arranged on a triangular pitch with a pitch-to-diameter ratio of 1.096. The fuel pins have a large diameter of 2.7 cm that provides a large hydraulic diameter for Pb coolant flow reducing the frictional pressure drop through the core as required for natural circulation. The core is a single open cassette of fuel pins and is not composed of individual removable assemblies.

Table1. SSTAR Core Conditions and Performance

Core Diameter, m	1.02
Active Core Height, m	0.8
Nitride Fuel Smeared Density, %	85
Fuel Volume Fraction	0.55
Cladding Volume Fraction	0.16
Bond Volume Fraction	0.10
Coolant Volume Fraction	0.16
Fuel Pin Diameter, cm	2.7
Fuel Pin Pitch-to-Diameter Ratio	1.096
Cladding Thickness, mm	1.0
Average Power Density, W/cm^3	69
Specific Power, KW/Kg HM	10
Peak Power Density, W/cm^3	119
Average Discharge Burn up, MWd/Kg HM	72
Peak Discharge Burn up, MWd/Kg HM	120
Peak Fast Fluence, n/cm^2	4.0×10^{23}
BOC to EOC Burn up Swing, % delta rho	0.13
Maximum Burn up Swing, % delta rho	0.36
Estimated Delayed Neutron Fraction	0.00375
BOC to EOC burn up Swing, $	0.35
Maximum Burn up Swing, $	0.96

4.0 REACTIVITY FEEDBACK COEFFICIENTS

The reactivity feedback coefficients that have been calculated for the SSTAR core are shown in Table 2 at the beginning of the 20-year core lifetime (BOC), the peak of the burn up swing (POC) occurring at approximately 13 years, and at the end of the lifetime (EOC). The delayed neutron fraction and prompt neutron lifetime are typical for a fast reactor fueled with TRU. The coolant density reactivity feedback coefficient is rather small. This is a result of the low coolant volume fraction in the core together with the low volume expansion coefficient of the Pb coolant. The change in sign of the coolant density reactivity feedback coefficient is a result of shifting of the location of the peak power. At the beginning of the core life, the power peaks in the outer portion of the core such that leakage dominates the effects of coolant density change. At the peak-of-cycle and at the end of the core life, the power peak has shifted into the center of the core where spectral effects dominate the effects of change in coolant density. The axial expansion and radial expansion reactivity feedback coefficients are large in magnitude reflecting the compactness of the core. The Doppler coefficient is typical for that of a fast reactor with TRU fuel. The relative size of the “flooded” and voided Doppler coefficients is somewhat surprising; work is in progress to investigate the source of this effect. The coolant void worth is negative. This is due to the small core size and the small coolant volume fraction. The void worth itself is not directly relevant to the calculation of system behavior because, as noted above, in all operational transients and postulated accidents, the core remains covered by single-phase liquid Pb.

Table 2. Reactivity Feedback Coefficients for SSTAR

	BOC	POC	EOC
Delayed Neutron Fraction	0.0035	0.0034	0.0034
Prompt Neutron Lifetime, s	1.8E-07	1.8E-07	1.8E-07
Coolant Density, cents/°C	-0.002	0.003	0.002
Fuel Density, cents/°C	-0.28	-0.28	-0.28
Structure Density, cents/°C	0.03	0.04	0.04
Core Radial Expansion, cents/°C	-0.16	-0.16	-0.16
Core Radial Expansion, $/cm	-2.35	-2.36	-2.35
Axial Expansion, cents/°C	-0.06	-0.06	-0.06
Axial Expansion, $/cm	-0.91	-0.94	-0.89
Doppler, cents/°C	-0.12	-0.12	-0.11
Voided Doppler, cents/°C	-0.14	-0.13	-0.13
Coolant Void Worth, $	-0.99	-0.45	-0.71

5.0 SYSTEM THERMAL HYDRAULIC DEVELOPMENT

Figure 3 shows the primary coolant system configuration. The Pb coolant flows upwards through the core and the above-core riser region interior to the above-core shroud. Coolant flows through the holes in the shroud and enters the modular in-reactor heat exchangers to flow downwards over the exterior of double-walled circular tubes arranged on a triangular pitch through which the S-CO_2 flows upwards. Heat is thus transferred from Pb to S-CO_2 in a countercurrent regime. The Pb exits the heat exchangers to flow downwards through the downcomer to enter the reactor vessel lower head. A flow distributor head provides for an approximately uniform pressure boundary condition beneath the core.

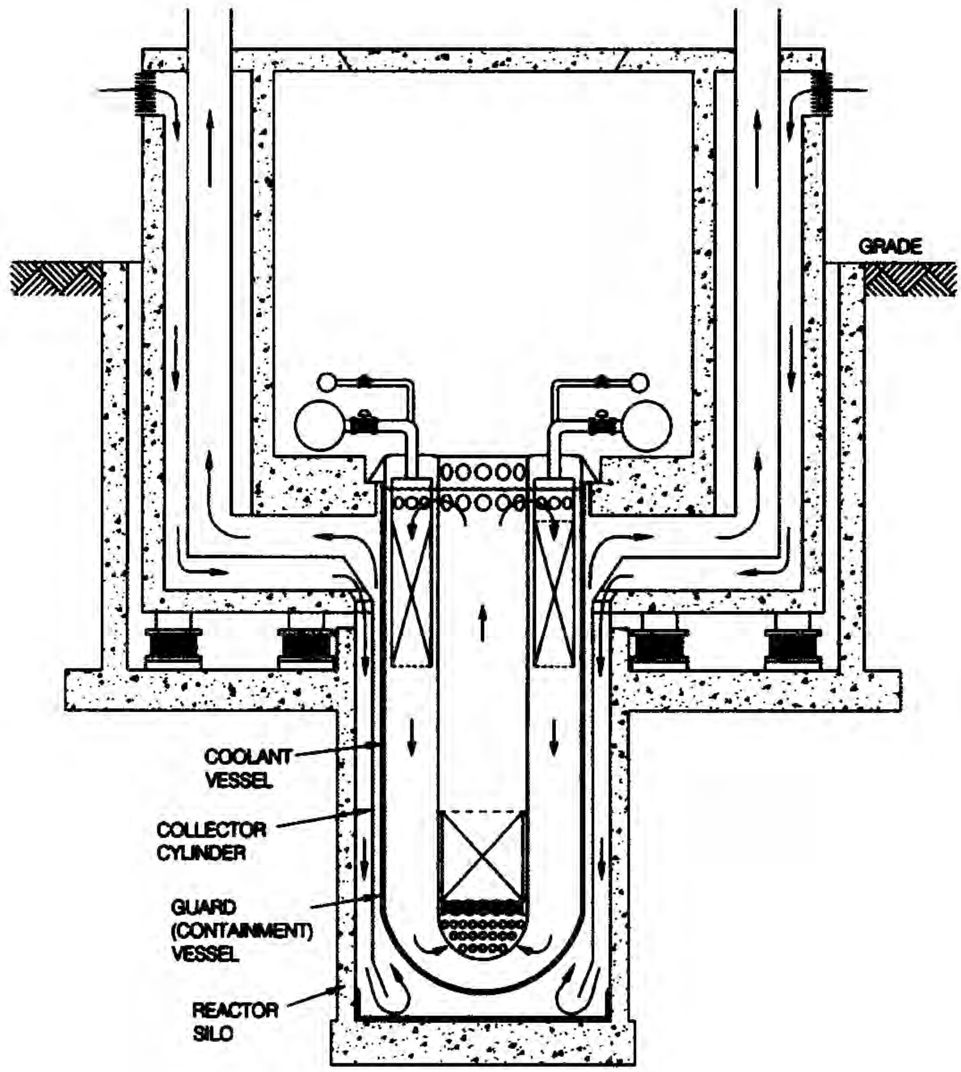

Figure 3. Illustration of SSTAR/LFR

The SSTAR reactor system thermal hydraulic development has been carried out to meet the following requirements and constraints:

- Power level = 45 MWt;
- Full transportability by barge or rail;
- Natural circulation heat transport of primary coolant at power levels up to and exceeding 100 % nominal;
- Core dimensions and fuel volume fraction from core neutronics analyses;

- Peak cladding temperature equal to 650 ☜C;
- Maximize S-CO_2 Brayton cycle efficiency;
- Fission gas plenum height above active core equal to 25 % of active core height;
- Pb coolant channels about 1 cm or more in diameter to reduce potential for plugging by contaminants;
- Space for incorporation of cylindrical liner and annular gap escape path for CO_2 vapor/gas between in-vessel Pb-to-CO_2 heat exchangers and reactor vessel inner surface;
- Space for multi-plate thermal radiation heat shield between bottom of upper head/cover and Pb free surface;
- Adequate coolant temperature margin above the freezing temperature;
- Heat removal of decay heat from outside of guard/containment vessel to the inexhaustible atmosphere heat sink by natural circulation of air.

Vessel size is constrained by conflicting goals. Rail transportability imposes a size limitation upon the reactor vessel and guard vessel of 6.1 m (20 feet) in diameter and 18.9 m (62 feet) in height. Alternately, the vessel height (18.3 m) and diameter (3.23 m) are determined by the need to fit the following components inside of the vessel and to provide sufficient driving head for single-phase natural circulation heat transport between the elevations of the in-reactor heat exchangers and the active core:

- 1.02 m active core diameter;
- 0.297 m reflector thickness;
- 2.54 cm core shroud thickness interior to downcomer;
- 5.72 cm thick gap between reactor vessel inner surface and 1.27 cm thick cylindrical liner to provide escape path to Pb free surface for CO_2 void, in the event of HX tube rupture;
- 5.08 cm thick reactor vessel;
- Kidney-shaped Pb-to-CO_2 heat exchangers must fit inside of annulus between shroud and reactor vessel, and provide sufficient heat exchange performance to realize a significant Brayton cycle efficiency.

The fission gas plenum height is based upon an assumed conservative gas release from nitride fuel of 2.5 % per atom % of burn up. The fuel volume fraction is held fixed in the thermal hydraulic design analyses at the value of 0.55 assumed by the core analyses.

The fuel rod outer diameter and pitch-to-diameter ratio were varied to determine an optimum combination. Figure 4 shows the relationship between pitch-to-diameter ratio and rod diameter for a triangular lattice with a fixed fuel volume fraction of 0.55 and a fixed fuel smeared density of 85 %.

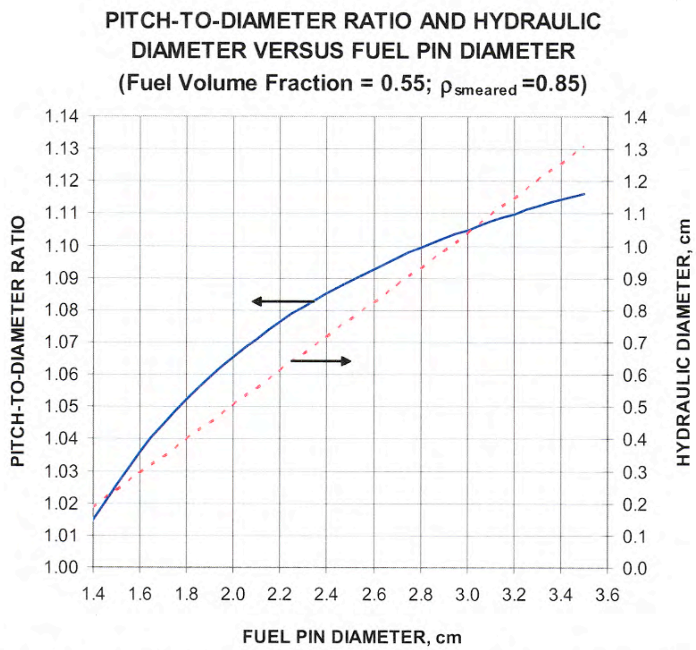

Figure 4. Relationship Between Fuel Pin Diameter and Triangular Pitch-to-Diameter Ratio.

Using this relationship, the fuel pin diameter is determined as the optimal value that minimizes the peak cladding inner surface temperature (assuming a 1.0 mm cladding thickness). Figure 5 shows the dependencies upon the fuel pin diameter and core inlet temperature with the frictional losses in the heat exchangers temporarily reduced. Dependencies of the core outlet temperature are presented in Figure 6. The heat exchanger tube height and pitch-to-diameter ratio are then determined to provide a 650 °C peak cladding temperature and to maximize the S-CO_2 Brayton cycle efficiency (Figures 7 and 8). Table 3 presents operating conditions for the 45 MWt SSTAR coupled to a S-CO_2 Brayton cycle.

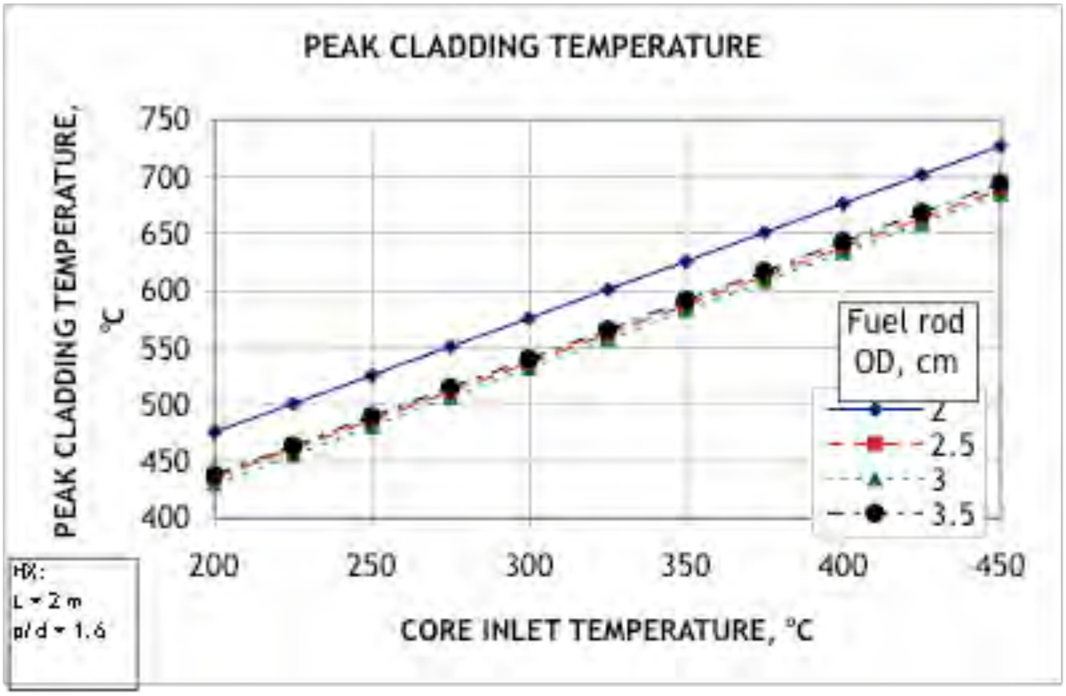

Figure 5. Dependencies of Peak Cladding Temperature Upon Core Inlet Temperature and Fuel Pin Diameter.

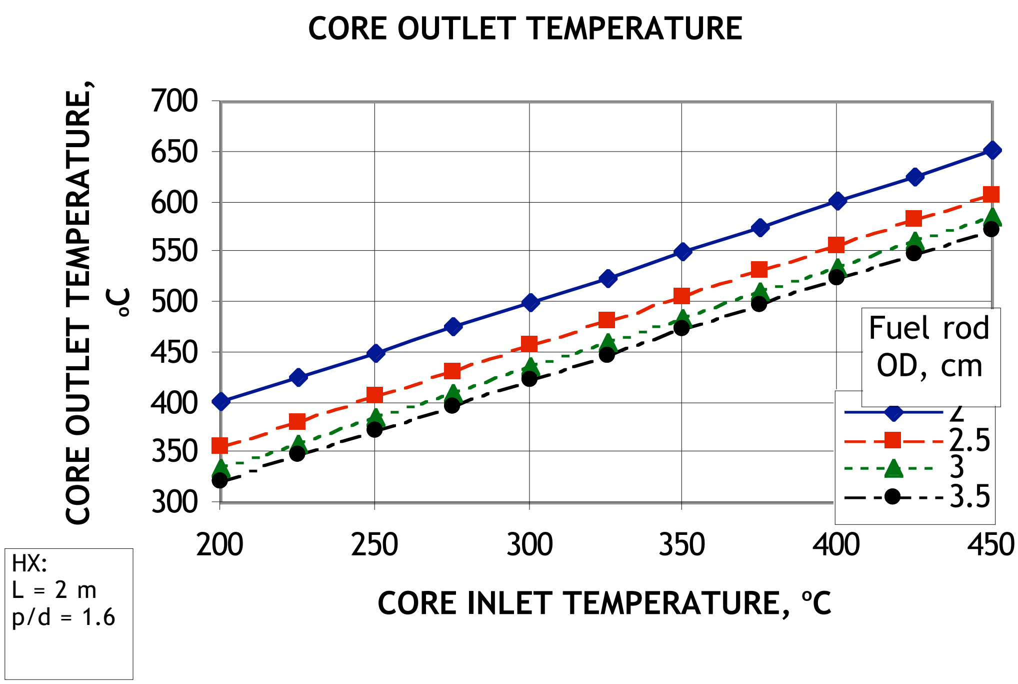

Figure 6. Dependencies of Core Outlet Temperature Upon Core Inlet Temperature and Fuel Pin Diameter.

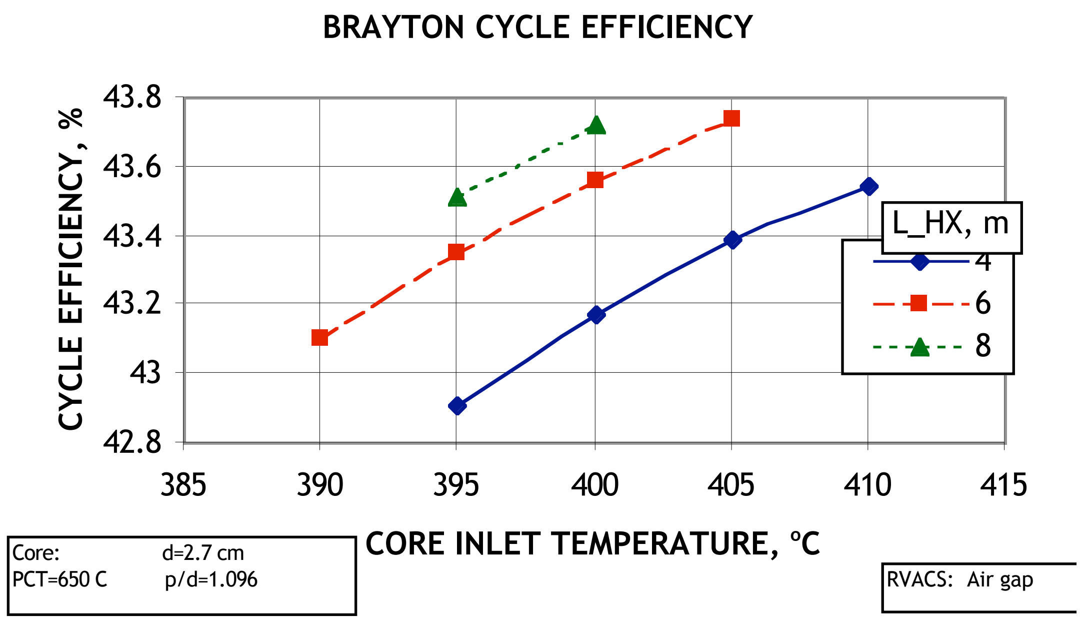
BRAYTON CYCLE EFFICIENCY
CYCLE EFFICIENCY, %
43.8
43.6
43.4
43.2
43
42.8
385
390
395
400
405
410
415
CORE INLET TEMPERATURE, °C
L_HX, m
4
6
8
Core: d=2.7 cm
PCT=650 C p/d=1.096
RVACS: Air gap

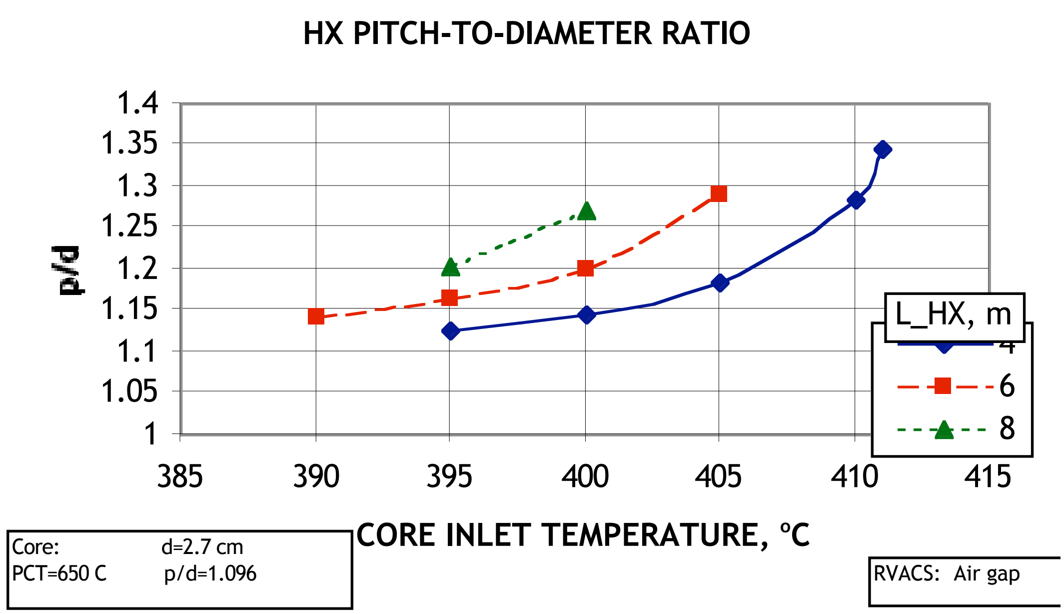
HX PITCH-TO-DIAMETER RATIO
p/d
1.4
1.35
1.3
1.25
1.2
1.15
1.1
1.05
1
385
390
395
400
405
410
415
CORE INLET TEMPERATURE, °C
L_HX, m
4
6
8
Core: d=2.7 cm
PCT=650 C p/d=1.096
RVACS: Air gap

Table 3. SSTAR Operating Conditions

Power, MWe (MWt)	20 (45)
Reactor Vessel Height, m (feet)	18.3 (60.0)
Reactor Vessel Outer Diameter, m (feet)	3.23 (10.6)
Active Core Diameter, m (feet)	1.02 (3.35)
Active Core Height, m (feet)	0.80 (2.62)
Active Core Height-to-Diameter Ratio	0.8
Fuel Volume Fraction	0.55
Fuel Pin Outer Diameter, cm	2.7
Fuel Pin Pitch-to-Diameter Ratio	1.096
Core Hydraulic Diameter, cm	0.876
Cladding Thickness, mm	1.0
Fuel Smeared Density, %	85
HX Tube Height, m	6.0
HX Tube Outer Diameter, cm	1.4
HX Tube Inner Diameter, cm	1.0
HX Tube Pitch-to-Diameter Ratio	1.302
HX Hydraulic Diameter for Pb Flow, cm	1.22
HX-Core Thermal Centers Separation Height, m	12.2
Peak Fuel Temperature, °C	1009
Peak Cladding Temperature, °C	650
Core Outlet Temperature, °C	561
Maximum S-CO_2 Temperature, °C	541
Core Inlet Temperature, °C	405
Core Coolant Velocity, m/s	0.948
Pb Coolant Flowrate, Kg/s	1983
CO_2 Flowrate, Kg/s	245
CO_2 Mass in Brayton Cycle, Kg	8737
S-CO_2 Brayton Cycle Efficiency, %	43.8
Plant Efficiency, %	43.4

The SSTAR reactor is coupled to a supercritical carbon dioxide (S-CO_2) Brayton cycle power converter that provides a greater cycle efficiency at the Pb outlet temperature and has smaller, simpler, and fewer components as well as a smaller plant footprint relative to the traditional Rankine steam cycle operating at the same reactor outlet temperature. The general features of the S-CO_2 Brayton cycle are discussed in the literature[2-4]. The present discussion shall therefore be limited to SSTAR-specific attributes. Figure 9 is a schematic of SSTAR coupled to the S-CO_2 Brayton cycle showing the heat transfer paths as well control mechanisms for the Brayton cycle. The turbine and two compressors are connected via a common shaft. This enhances the cycle efficiency and reduces the required generator power. Conditions for the turbine and compressors are presented in Table 4; the turbo machinery components are observed to have remarkably small sizes. The power conversion plant also incorporates a shutdown cooling compressor to circulate CO_2 through the in-reactor heat exchangers and a shutdown cooler to remove decay heat while allowing S-CO_2 Brayton cycle components to be isolated for maintenance or repair.

The two recuperators and cooler are assumed to consist of Printed Circuit Heat Exchangers (PCHEs) in which millimeter-scale semi-circular channels are chemically etched into plates that are subsequently hot isostatically pressed together at high temperature and pressure. Use of PCHEs offers the potential for savings in the recuperator and cooler volumes relative to shell-and-tube heat exchangers. For the present analysis, it is assumed that the etched-plate manufacturing process limits the plate width to 0.6 m. To obtain the required heat exchange area, twelve such PCHEs are incorporated to realize each of the high temperature recuperator (HTR), low temperature recuperator (LTR), and cooler heat exchanger units. A concept was developed whereby the three components are assembled from three transportable modules. Each module consists of twelve PCHEs in total: four 2.0 m long PCHEs belonging to the high temperature recuperator (located at the top); four 2.0 m long PCHEs belonging to the low temperature recuperator (in the middle); and four 1.6 m long PCHEs of the cooler (at the bottom). A steel space frame supports the PCHEs.

Pressures and temperatures for the Pb and S-CO_2 circuits are shown on the schematic in Figure 10.

Table 4. Results of Turbine and Compressor Analyses for 45 MWt SSTAR

	Turbine	Compressor No. 1	Compressor No. 2
Power, MW	31.1	4.88	5.80
Number of Stages	5	10	10
Length without Casing, m	0.41	0.27	0.13
Maximum Diameter without Casing, m	0.37	0.15	.21
Minimum Hub Diameter, m	0.210	0.106	0.184
Maximum Hub Diameter, m	0.286	0.116	0.204
Minimum Blade Height, cm	3.1	1.3	0.6
Maximum Blade Height, cm	4.5	1.9	1.1
Minimum Blade Chord, cm	3.4	1.2	0.6
Maximum Blade Chord, cm	5.2	1.5	0.8
CO_2 Flowrate, Kg/s	245	164	80.8
Efficiency without Secondary Losses, %	96.0	92.5	90.5
Assumed Secondary Losses, %	5.0	5.0	5.0
Net Efficiency, %	91.0	87.5	85.5

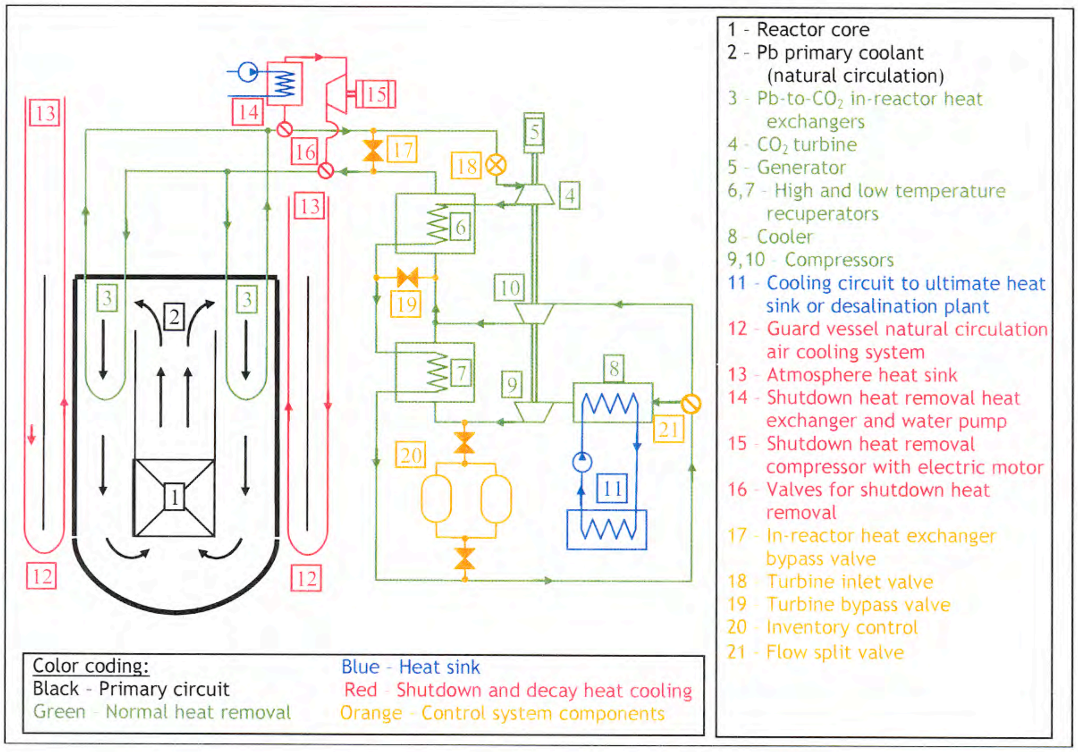

Figure 9. Schematic Illustration of SSTAR Coupled to the S-CO_2 Brayton Cycle Showing Normal, Shutdown, and Emergency Heat Transfer Paths.

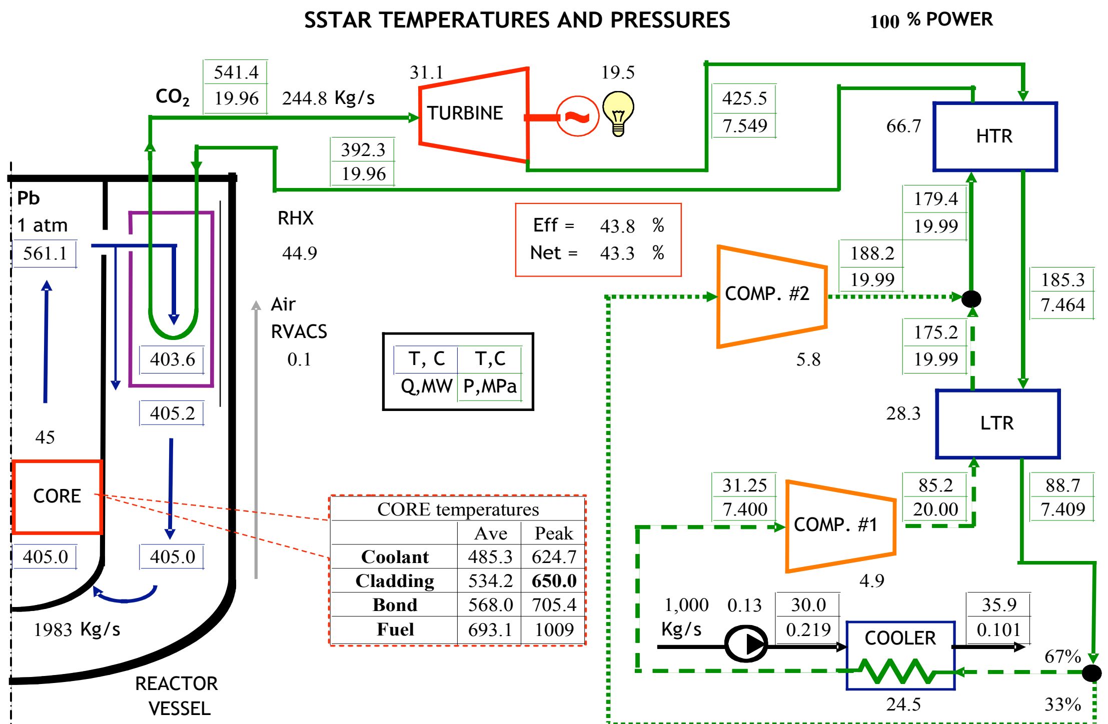

Figure 10. Schematic Illustration of SSTAR Coupled to S-CO_2 Brayton Cycle Showing Temperature, Pressures, and Heat Exchange Rates.

6.0 SUMMARY OF SSTAR DEVELOPMENT

Results of Pre-conceptual core neutronics and system thermal hydraulics calculations indicate that a SSTAR Pb-cooled, proliferation resistant, natural circulation, small modular fast reactor concept with a 20-year core lifetime, good core reactor physics performance, and a high plant efficiency of 43 % (S-CO_2 gas turbine Brayton cycle efficiency of 44 %) may be viable at an electrical power level of 20 MWe (45 MWt). In particular, the SSTAR concept achieves a maximum average discharge burn up of 72 MWd/Kg HM, a maximum burn up reactivity swing during the 20 year core lifetime of less than one dollar, and a mean core temperature rise of 156 °C while the peak cladding structural temperature is limited to 650 °C.

7.0 PUBLICATIONS

The following draft full-length papers have been prepared during the reporting period:

W. S. Yang, M. A. Smith, A. V. Moisseytsev, J. J. Sienicki, and D. C. Wade, "Lead-Cooled, Long-Life Fast Reactor Design for Remote Deployment," 2005 International Conference on Advances in Nuclear Power Plants, ICAPP 2005, Seoul, May 15-19, 2005.

J. J. Sienicki and A. V. Moisseytsev, "SSTAR Lead-Cooled, Small Modular Fast Reactor for Deployment at Remote Sites-System Thermal Hydraulic Development," 2005 International Conference on Advances in Nuclear Power Plants, ICAPP 2005, Seoul, May 15-19, 2005.

8.0 REFERENCES

1. J. J. Sienicki, M. A. Smith, A. V. Moisseytsev, W. S. Yang, and D. C. Wade, "Interim Status Report on Pre-conceptual Core and System Thermal Hydraulic Studies for the SSTAR/LFR Small Modular Fast Reactor," Deliverable Report Prepared for WBS No. 1.05.01, Work Package No. A0501J01, Lead Fast Reactor, System Design and Evaluation-ANL, Generation IV Nuclear Energy Systems, Argonne National Laboratory, August 30, 2004.
2. V. Dostal, M. J. Driscoll, P. Hejzlar, and N. E. Todreas, "A Supercritical CO_2 Gas Turbine Power Cycle for Next Generation Nuclear Reactors," ICONE 10-22192, Proceedings of ICONE10, Tenth International Conference on Nuclear Engineering, Arlington, April 14-18, 2002.
3. A. V. Moisseytsev, J. J. Sienicki, and D. C. Wade, "Cycle Analysis of Supercritical Carbon Dioxide Gas Turbine Brayton Cycle Power Conversion System for Liquid Metal-Cooled Fast Reactors," ICONE11-36023, 11th International Conference on Nuclear Engineering, Tokyo, April 20-23, 2003.
4. A. V. Moisseytsev, J. J. Sienicki, and D. C. Wade, "Turbine Design for a Supercritical Carbon Dioxide Gas Turbine Brayton Cycle," Paper 3064, Proceedings of ICAPP '03, 2003 International Congress on Advances in Nuclear Power Plants, Córdoba, Spain, May 4-7, 2003.

Coolant & Material Studies

Use of lead or LBE coolant results in unique materials challenges and R&D needs. Coolant properties and coolant handling technologies must be developed for reliable operation, including coolant chemistry control as well as fundamental thermo-hydraulic properties. In addition, materials will face operational and reliability challenges including extended corrosion resistance in liquid lead or LBE, significant fast neutron exposure and mechanical stability at temperatures at or above past experience

Materials Requirements: B. Halsey (LLNL):
Work is underway to update the initial component/materials matrix later this year to address higher temperatures and to consider more advanced 'developmental' materials systems.

Corrosion Testing: M. Williamson (ANL)
Tests are continuing of compatibility of candidate structural materials with lead and lead-bismuth eutectic. At the end of FY04, samples were obtained of the ODS alloy MA957 that had been exposed in a flowing loop-type experiment to lead at temperatures of 800C (hot leg) and 650C (cold leg). Microscopic examination of the samples is continuing during the present reporting period but preliminary results are encouraging in that minimal deterioration of the samples has so far been observed. To obtain comparable results with Pb-Bi a test is currently in progress that has exposed MA957 samples to the same temperature gradient but in Pb-Bi. This test will be terminated shortly and microscopic examination of the samples will be undertaken. This will provide a valuable comparison of the relative corrosiveness of the two potential heavy metal coolants with the same test alloy. (MAW)

Corrosion Testing: N. Li (LANL)
We performed several corrosion test campaigns in DELTA at LANL in the last year. The latest is a 400-hr test at 520 deg C, with about 1.5 m/s LBE flow velocity. The oxygen concentration was measured and adjusted, and varied around the target level of 10^-6 wt%. The materials tested include 316L, HT-9, 9Cr-1Mo, EP823, several Fe-Cr-Si and Fe-Si alloys, and surface modified steels – aluminized 316L (from CEA), and shot-peened 316L. The specimens were analyzed with SEM.

The efficacy of higher Cr and Si on enhancing corrosion resistance is confirmed from the analysis. Aluminized 316L also performed well with no obvious corrosion observed. While shot peening (introducing cold work and compression) did alter the oxidation formation, such type of surface modification appears insufficient by itself. Alloy composition modification and/or coating may be necessary to achieved sufficient corrosion resistance for long-term applications in LFRs. Alumina specimens were completely impervious to LBE at this temperature, as expected.

Based on these and other reported test results, we are developing a Fe-Cr-Si alloy for a weld overlay over reactor-ready structural materials (e.g. HT-9 and mod 9Cr-1Mo) for enhanced surface corrosion resistance without compromising radiation resistance of the substrate materials. Procurement of several experimental heats of alloys and welding rods is coordinated with UNLV and MIT.

Corrosion Modeling: N. Li (LANL)
At LANL we incorporated the oxidation growth and removal by liquid metal flow into our system kinetic model, and estimated the rate constants based on the Wagner theory for oxidation and the mass transfer corrosion in liquid metals. The model is benchmarked against earlier 3000 hr LBE loop test data for HT-9 and D9 with reasonable agreement. The most significant finding is the characterization of early stage corrosion dominated by oxidation, and asymptotic long-term corrosion dominated by mass transfer corrosion through the protective oxide layer. The model produces the key features and provides the framework to systematically screen candidate materials for short durations and predict long-term corrosion rate, which is missing from most international test data up till now. We developed a corrosion test reporting protocol based on our modeling work and distributed to the OECD/NEA LBE working group for comment.

The system kinetic model naturally contains precipitation from transport of corrosion products. This feature is benchmarked against a JAERI LBE loop experiment with good agreement. We have extracted sections of piping from DELTA in the ongoing upgrading effort and will analyze them for further validation of the corrosion model.

Recent Publications:

"Dynamics of High Temperature Oxidation Accompanied by Scale Removal and Implications for Technological Applications", J. Zhang, N. Li and Y. Chen, accepted for publication in Journal of Nuclear Materials (2005).

"Corrosion behaviors of US steels in flowing lead–bismuth eutectic (LBE)", J. Zhang, N. Li, Y. Chen and A. Russanov, Journal of Nuclear Materials, 2005, 336, 1-10.

"Corrosion/precipitation in non-isothermal and multi-Modular LBE Loop", J. Zhang, N. Li, Journal of Nuclear Materials, 2004, 326, 201-210.

"Analytical Solution on Transient Corrosion/Precipitation in Closed Loop Systems", J. Zhang, N. Li, Corrosion, 2004, 60(4). 331-341.

"A Correlation of Steel Corrosion in Non-isothermal LBE Loop Systems", J. Zhang, N. Li, Journal of Nuclear Science and Technology, 2004, 41(3). 260-264.

Coolant Technology: N. Li (LANL)
The direct gas (H2 or O2 mixed with He) injection system to adjust oxygen without automation (due to safety concerns) is insufficient for steady state oxygen control due to slow system response. We obtained PbO pellets and began to add a cold variable temperature bypass line to DELTA that will use the dissolution and precipitation of PbO to function as a solid mass exchanger for equilibrium oxygen concentration control. We will test the performance of such implementation and make improvement later this year.

We continue to work with MIT and I-NERI collaborators of Seoul National University to improve the sealing of oxygen sensors via metal-ceramic brazed joints. In addition, we are testing Pt/air reference electrode for higher temperature services.

We hosted an INL staff at LANL to begin the transfer of our LBE technology and operating experience, and the planning of an engineering-scale lead test facility to elevate the coolant technology to the maturity level suitable for test/demo reactor design and construction.

Amorphous Metal Testing - B. Halsey (LLNL):
A modest effort is underway to explore the potential for amorphous metal application in LFR systems, leveraged from an ongoing R&D program co-funded by other agencies (DARPA and OCRWM). Rather than development of an entirely new material, we are obtaining samples of existing amorphous metal that has a composition similar to some of the current LFR candidate F-M steels. (DAR40 (Fe52.3Mn2Cr19Mo2.5W1.7B16C4Si2.5)). Initial samples should be ready for lead and LBE corrosion testing within a few months.

Systems Studies

Critical Path R&D:
A re-evaluation of critical path R&D is underway to optimize resource use while developing an adequate basis for a future decision to proceed to a demonstration.

Regulatory Approach: N. Brown (LLNL)
The so-called "license-by-test" approach continues to be the preferable approach to licensing the LFR design. We have identified based on review of the Galena, AK Toshiba initiative that small sites may not fit neatly into the vision we have for regulation of small reactors. Single small reactors serving small communities and small utilities may not qualify as nuclear operators from a nuclear liability standpoint. Nuclear operators typically require liability limits that make it possible to buy affordable insurance and be protected in the event of a severe accident. Small rural utilities may have difficulty qualifying for the limited liability provided by laws such as Price-Anderson. There are likely to be ways to address the issue, but it's another factor that will need consideration. The Galena initiative's interaction with the NRC may provide some guidance on how the issue can be addressed.

International Cooperation

LFR GIF System Steering Committee: C. Smith (LLNL)
An initial meeting to form an LFR Steering Committee of the GEN-IV International Forum (GIF) was held in Genoa on 19 October 2004 with representatives from the US and Euratom.

The main objectives of the meeting were:

- to exchange information on the present status of LFR development in US and Europe;
- to identify a near term program of activities to initiate the LFR Steering Committee.

Following the meeting, contact was made with designated member of the LFR-SC from Japan, and also with a prospective member from South Korea. The first formal meeting of the full committee is being planned for February or March, 2005 in Monterey, CA.

CRIEPI Cooperation: N. Brown (LLNL)
LLNL has continued as the focal point for the LFR project's communication with CRIEPI and the research on small liquid metal reactors in Japan, particular their 4S design. Dr. Minato from CRIEPI has been on assignment at LLNL since March of 2004. Safety issues common to small sodium and lead cooled reactors and the economics associated with these types of reactors has been the focus of his research. Detailed cost data generated by the PRISM project are being used to develop a cost model for both small sodium and lead cooled power reactors.

Safety issues common to both types of small reactors include among others: sodium void reactivity design requirements, containment design basis, potential for void bubbles passing through the core, running fuel beyond clad breach in a sealed reactor, and the choice of reactivity control mechanisms. These topics are being considered during FY-04

Conclusion

A phased program for reactor design is underway in parallel with coolant and material R&D, selection and qualification and fuel development to support a decision on construction of a demonstration system within ten years.